Seasonal and interannual variations of Amur River discharge and their relationships to large-scale atmospheric patterns and moisture fluxes

Yoshihiro Tachibana[1,2], Kazuhiro Oshima[3] and Masayo Ogi[4,5]

[1] Institute of Observational Research for Global Change, Japan Agency for Marine-Earth Science and Technology, Yokosuka, Japan. E-mail: tachi@bio.mie-u.ac.jp
[2] Faculty of Bioresources, Mie University, Tsu, Japan
[3] Faculty of Environmental Earth Science, Hokkaido University, Sapporo, Japan
[4] The Joint Institute for the Study of the Atmosphere and Ocean, University of Washington, Seattle, WA, USA
[5] Frontier Research Center for Global Change, Japan Agency for Marine-Earth Science and Technology, Yokohama, Japan

Abstract

Using reanalysis data, we investigate the relationship of Amur River discharge and vertically integrated atmospheric horizontal moisture flux. The discharge has two peaks, one in spring and the other in autumn. A northward flux associated with storms in the previous autumn and winter contributes to the spring discharge. The autumn discharge is supplied by a northward flux associated with the Asian summer monsoon and by an eastward flux originating from evaporation in Eurasia. Interannual variation is also investigated. The strong summer monsoon strengthens the summer flux convergence, resulting in anomalously large discharge in autumn. The strong winter monsoon wind with a dry air mass activates evaporation. The anomalously large spring discharge is related to the warm phase of the Arctic Oscillation. These results indicate that the monsoon plays an important role in the freshening of the Okhotsk Sea.

This work is partially based on a paper by Tachibana, Oshima and Ogi (2008) in the *Journal of Geophysical Research.* See this paper for details.

Introduction

The Amur River, with a basin area of 1.86×10^6 km^2, is the fourth largest river in northern Eurasia and supplies much of the fresh water to the Okhotsk Sea, one of the southernmost ice-covered seas in the Northern Hemisphere. Freshwater discharge from the Amur River, which causes large stratification that suppresses deep convection and promotes freezing, is an important factor controlling the formation of sea ice in the Okhotsk Sea.

According to Ogi *et al.* (2001), the annual amount of discharge from the Amur River is 333 km^3/year (10,929 m^3/s). A distinctive characteristic of the seasonal cycle of the Amur River is its two discharge peaks, one in June and the other in September (Fig. 1a). The Amur River is the only river in northern Eurasia to have double discharge peaks (Masuda, 2007, pers. comm.). Ogi *et al.* (2001) speculated that the first peak occurs due to melting snowpack and frozen soil, whereas the second peak is caused by summertime monsoon precipitation.

Past studies have commonly applied vertically integrated horizontal moisture flux analysis, using reanalysis and river discharge data, to rivers flowing toward the Arctic. This method might indicate the origins of the moisture that becomes river discharge. According to a tagged water experiment using an atmospheric general circulation model simulation by Numaguti (1999), the summer precipitation in northern Eurasia originates partially from water vapor that evaporates from inland areas of the Eurasian continent. However, because of the lack of detailed study of the moisture flux associated with the Amur River, the moisture source remains unclear.

Few papers have described the interannual variability of the Amur River. Ogi and Tachibana (2006) found that the interannual variation in the Amur River discharge is related to the annual mean Northern Hemisphere Annular Mode/Arctic Oscillation (NAM/AO). However, because there are two peaks in the discharge, the large-scale atmospheric patterns and local-scale storm tracks governing the spring

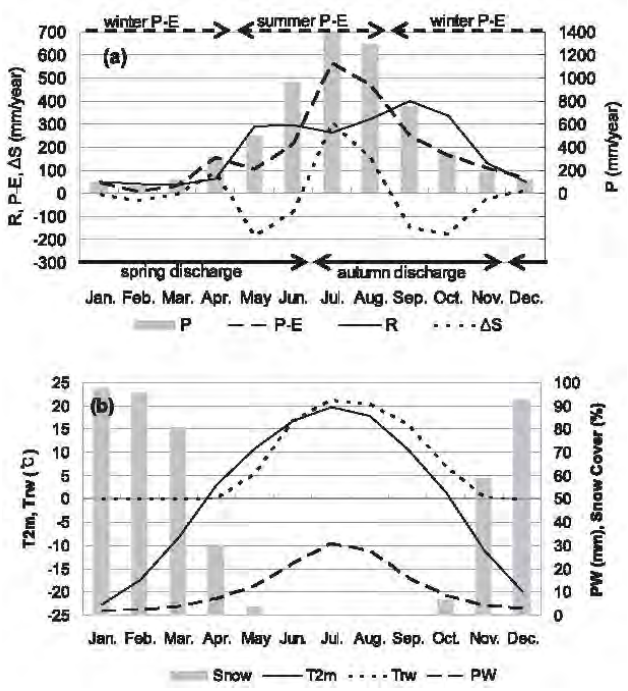

Fig. 1 (a) Seasonal cycle of the Amur River discharge (solid line), net precipitation (dashed line), precipitation from APHRODITE (www.chikyu.ac.jp/precip/; gray bars) and $\partial S/\partial t$ (dotted line) over the Amur River basin. (b) Other climatological conditions over the basin; temperature at 2 m (solid line), river water temperature (dotted line), snow cover (gray bars) and PW (precipitable water; dashed line).

discharge peak must differ from those governing the autumn peak. However, no previous studies have clarified the large-scale atmospheric patterns and local-scale storm tracks that determine individual discharge peaks.

The purpose of this study is to determine which atmospheric patterns govern the spring and autumn discharge peaks. We will illustrate the origin of the moisture. Moreover, we will determine the interannual variations in the atmospheric patterns that influence the two discharge peaks.

Data and Methods

Monthly mean Amur River discharge data from 1980 through 2001 are used for the analysis. These data were recorded at Bogorodskoe, the lowest-reach hydrological station of the Amur River at which discharge has been routinely measured by the Far Eastern branch of the Russian Federal Service for Hydrometeorology and Environmental Monitoring (FERFSHEM).

Data from the European Centre for Medium-Range Weather Forecasting is used to perform a 40-year reanalysis (ERA40) (Uppala *et al.*, 2005). The time resolution of the data is 6 hourly. The horizontal resolution is 2.5° latitude × 2.5° longitude. The analysis period is from 1979 through 2001.

We estimated the net precipitation (precipitation minus evaporation, $P - E$) over the Amur River basin from moisture flux. $P - E$ is estimated using the atmospheric moisture budget equation as follows:

$$\frac{\partial PW}{\partial t} = -\nabla \langle q\mathbf{v} \rangle + E - P, \qquad (1)$$

where PW is precipitable water, q is the specific humidity, $\mathbf{v}$ is the wind vector, and $\langle q\mathbf{v} \rangle$ represents the vertically integrated horizontal moisture flux. $P - E$ is estimated from the area-weighted average values of PW and the horizontal convergence of $\langle q\mathbf{v} \rangle$ over the area of the Amur River basin (Fig. 2).

Water vapor in the mid-latitudes is transported by both atmospheric stationary waves and moving transient eddies. Because the temporal scales of these two transports are quite different, dividing the moisture flux into these two categories provides useful information on the atmospheric causes of the discharge (Oshima and Yamazaki, 2006). We divide the monthly mean total moisture flux into stationary flux and transient flux as follows:

$$\langle \overline{q\mathbf{v}} \rangle = \langle \overline{q}\,\overline{\mathbf{v}} \rangle + \langle \overline{q'\mathbf{v}'} \rangle, \qquad (2)$$

where the overbars represent the monthly average, and the primes represent the deviation from the monthly average. The stationary flux is calculated from the monthly mean fields of wind, moisture, and surface pressure. The transient flux is obtained by subtracting the stationary flux from the total flux.

The connectivity of the $P - E$ and the river discharge R is described using the terrestrial water budget equation. The time rate of change in land water storage S is written as:

$$\frac{\partial S}{\partial t} = P - E - R, \qquad (3)$$

where R is the river runoff. Thus, R is determined by $\partial S/\partial t$ and $P - E$.

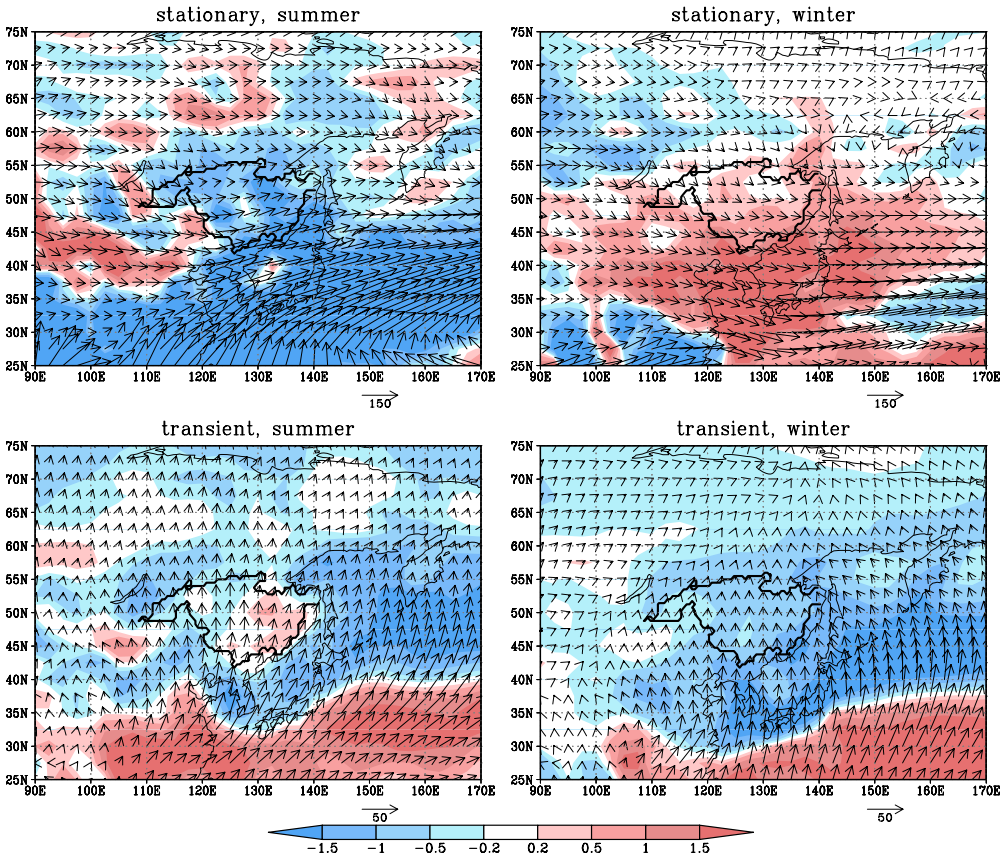

Fig. 2 Moisture flux and its divergence fields for the stationary (upper panels) component and transient (bottom panels) component in association with the summer $P - E$ (left panels) and winter $P - E$ (right panels).

Comparison of Discharge with Net Precipitation

Seasonal cycle of discharge and net precipitation

We compared the Amur River discharge with the $P - E$ estimated by the ERA40. The annual mean $P - E$ (182 mm/year) is close to the observed annual discharge (190 mm/year). The seasonal means and the interannual variation of $P - E$ are also close to those of the discharge, as will be shown later.

As discussed earlier, the river discharge has two discharge peaks, in June and September, while a single peak in $P - E$ occurs in July that is approximately 2 months later than discharge in autumn. This time lag of the autumn discharge peak behind the $P - E$ peak is related to the fact that runoff takes approximately 2 months to reach the outlet of the basin, given the massive size of the Amur River basin. Figure 1b shows several climatological conditions over the Amur River basin. The temperature at 2 m height changes from negative to positive in April and back to negative in October. This indicates that precipitation accumulates as snow from October to March and that the accumulated snow and frozen soil start to melt in April. The river water temperature has a seasonal cycle similar to that of temperature at 2 m height. The river water temperature becomes positive in May, indicating that frozen river water begins to melt in this month. The river water temperature falls to zero in November, and the river starts to freeze. Satellite observations indicate maximum snow coverage in January, a large decline beginning in April, and accumulation starting again in October. This suggests that snowmelt starts in April and that the discharge peaks in May to June with the decrease in storage.

To compare the discharge with moisture flux and atmospheric patterns in association with the two discharge peaks, we first confirm the months of $P - E$ that cause the respective spring and autumn discharge. Based on the two clear discharge peaks, we define December through June as the months of

spring discharge and July through November as the months of autumn discharge (Fig. 1a). We determined the periods of summer $P - E$ and winter $P - E$ that correspond to the spring and autumn discharge, respectively. From a procedure for the definition of the period in Tachibana *et al.* (2008), the time averaged $P - E$ from May through August (summer $P - E$) corresponds to the autumn discharge, and that from September through April (winter $P - E$) corresponds to the spring discharge (Fig. 1a). The summer $P - E$ (113) and winter $P - E$ (69) closely agree with the spring discharge (121 mm/year) and autumn discharge (69 mm/year), respectively.

Moisture flux patterns in association with summer $P - E$ and winter $P - E$

We compare the seasonal cycles of the moisture flux convergence and the $P - E$ over the Amur basin (Figure not shown). The seasonal $P - E$ cycle is similar to that of the moisture flux convergence, except in spring and autumn due to the large changes of PW (Fig. 1b). The stationary component of the moisture flux convergence is dominant in summer. Therefore, the moisture is transported mainly by stationary waves. In the winter, the transient component of the moisture flux convergence is positive and plays a principal role in supplying the water vapor in the Amur basin, while the stationary component is negative.

These characteristics are shown in the moisture flux fields associated with the summer $P - E$ and winter $P - E$ (Fig. 2). In summer, the northeastward flux of the stationary component mainly determines the total flux convergence. The flux from the East China Sea to Japan indicates the rain belt that coincides with the Baiu/Meiyu stationary front, in association with the Asian summer monsoon. Therefore, the summer flux is partially influenced by the Asian summer monsoon. The eastward flux from the west of the basin, which can be caused by mid-latitude westerlies, also contributes to the precipitation. Divergent areas are located in the far western inland area of the continent. Because the divergent area indicates that surface evaporation exceeds precipitation, the figure implies that water vapor which evaporates from inland areas also supplies precipitation to the Amur basin. This is consistent with a model study by Numaguti (1999).

In winter, the flux by the transient component converges over the Amur basin, whereas the flux by the stationary component diverges. The flux convergence of the transient component can be caused by storm activity in this season and region, where wintertime cyclones are known to begin and develop. The fluxes of the transient component suggest that the river water in the spring discharge originates from the Pacific, although these arrows are not the same as the material trajectories. In contrast, the fluxes of the stationary component around the Amur basin point southeastward. This direction is associated with the winter monsoon that blows from the cold, dry Eurasian continent toward the warm Pacific Ocean. Evaporation due to the stationary component associated with the dry monsoon wind over the Amur basin can cause the moisture flux divergence. Overall, the total flux in winter slightly converges over the Amur basin because of a larger moisture flux from the south by the transient component rather than by the stationary component.

Interannual Variation of Discharge

Interannual variation and its relationship to horizontal moisture flux patterns

Next, we investigate the causes of interannual variation in Amur River discharge. We compared the time series of spring and autumn discharge and their associated winter and summer $P - E$, respectively. Correlation coefficients are 0.84 for autumn discharge and summer $P - E$, and 0.57 for spring discharge and winter $P - E$. The large correlation for autumn discharge indicates that summer atmospheric processes principally govern autumn discharge. On the other hand, spring discharge is influenced not only by atmospheric processes related to the $P - E$, but also by other hydrological processes that are affected by variation in water storage S.

The variations in the total moisture flux convergence correlate well with the stationary components in both seasons. Thus, the stationary components are the prime determinant for the interannual variation in discharge. Now, we examine the stationary moisture flux in association with the interannual variation in spring and autumn discharge (winter and summer $P - E$). Figure 3 shows the composite maps of the stationary moisture fluxes in years of large (top 5) and small (bottom 5) summer $P - E$. Moisture flux fields in the top 5 years show counterclockwise circulation centered in the west of the basin. This indicates that the moisture tends to come from the Pacific to the southeastern Amur basin. In contrast, the flux in the bottom 5 years is more zonal than in

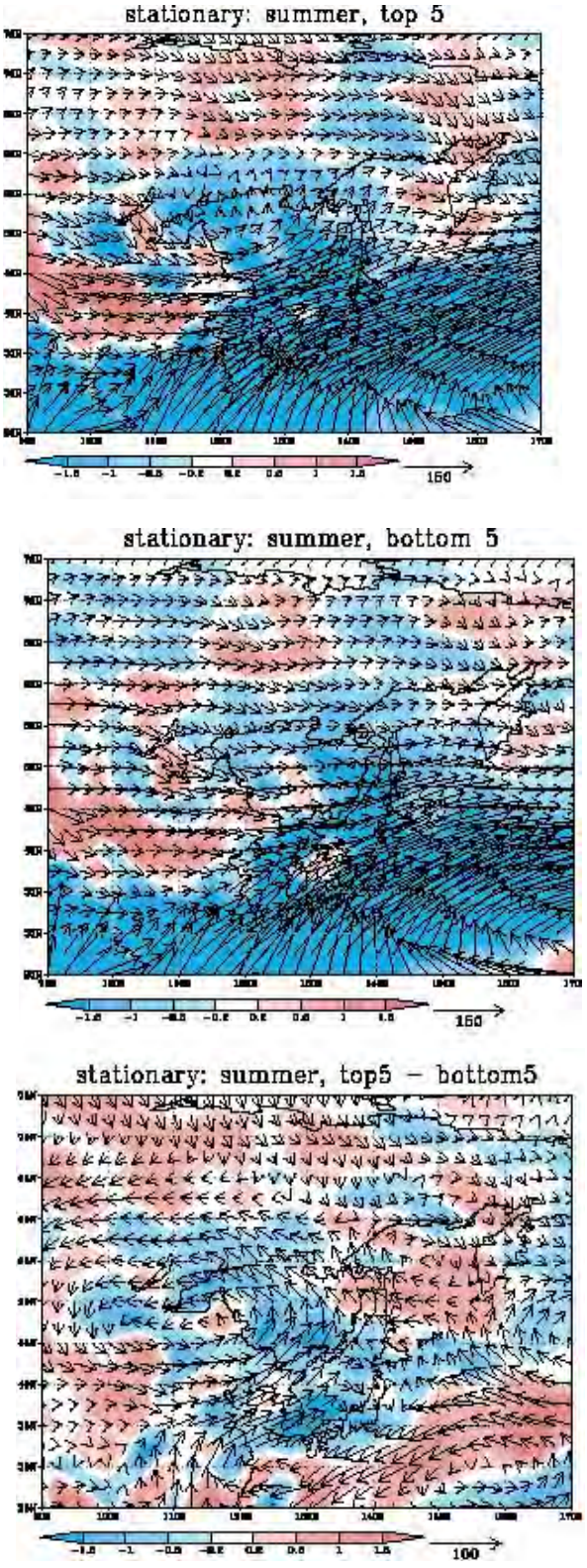

Fig. 3 Composite maps of the stationary moisture flux and its divergence in (top) the top 5 summer *P*– *E* years and (middle) bottom 5 years; (bottom) difference between the top 5 and bottom 5 years.

the top 5 years. The source region of the water in the bottom 5 years is thus mainly in inland continental areas. Figure 3 also shows the flux difference between the top 5 and bottom 5 years. A counterclockwise anomalous moisture flux pattern is obvious, suggesting that anomalous moisture flux from Southeast Asia also promotes anomalous *P* – *E* in the Amur basin, which then leads to anomalous autumn discharge.

In winter, on the other hand, the differences in the flux fields between the top 5 and bottom 5 years exhibit a counterclockwise circulation pattern centered to the west of the Amur basin (Figure not shown). The counterclockwise pattern and the overall northward orientation in the Amur basin suggest the weakness of the Asian winter monsoon.

Interannual variation and its relationship to large-scale atmospheric patterns

Large-scale atmospheric fields linearly regressed onto the interannual variation in the stationary component of the moisture flux convergence show that a notable feature in the circum-Amur basin area in summer is the presence of negative anomalies over the west of the basin (near Lake Baikal) in the sea level pressure (SLP), 500-hPa, and 200-hPa height fields, signifying a barotropic structure. Cold anomalies can be also seen around Lake Baikal (Figure not shown). The location of the cyclonic circulation anomaly in association with the cold anomalies is located just to the west of the Amur basin. This cyclonic circulation agrees with the counterclockwise moisture flux pattern of the stationary component in the years of large summer *P* – *E* (Fig. 3). Also, positive anomalies over the Okhotsk Sea can be seen in the SLP field. These anomalies are related to the appearance of the Okhotsk High. The contrast between the anomalous low pressure over land and the anomalous high pressure over the Okhotsk Sea brings about a northward moisture flux in association with northward wind anomalies in the lower troposphere over the Amur basin. This northward wind can then supply the Amur basin with moisture in association with the strengthened Asian summer monsoon. A west-to-east wavy pattern crossing the Eurasian continent at approximately 40° N, along the core of a subtropical westerly jet, is clearly visible at 200-hPa height. This wave train is possibly a stationary Rossby wave that originated over western Europe. The cyclonic circulation around Lake Baikal, which

directly influences the discharge, is thus related to this hemispheric mid-latitude circulation.

Winter atmospheric patterns associated with the winter flux of the stationary component have a continent-to-ocean contrast in the SLP field similar to that in summer. Significant positive SLP anomalies widely cover the Okhotsk and Bering seas, signifying the weakness of the Aleutian Low. Also, over Lake Baikal, significant negative anomalies appear in the SLP field. This feature implies a weakness of the winter Siberian High. Weakness of both the Siberian High and Aleutian Low causes weakening of the Asian winter monsoon, which usually blows from the continent to the Pacific. This atmospheric pattern is consistent with the moisture flux pattern in winter. The weak winter monsoon wind over the Amur basin can suppress the evaporation there. For this reason, the moisture flux divergence over the basin in the top 5 years can be weaker than in the bottom 5 years.

In addition, a hemispheric-scale pattern shows negative anomalies in the Arctic and positive anomalies in mid-latitudes from the surface to the upper troposphere at 200-hPa height, although statistical significance is low. These anomaly patterns are similar to the pattern of the positive phase of NAM/AO. This indicates that the NAM/AO pattern tends to be positive in winter with the large moisture flux. The positive phase of the NAM/AO is related to the weakened eastern Asian winter monsoon. Therefore, the relationship between this large moisture flux and the positive phase of NAM/AO is consistent with previous studies.

Summary

Using long-term discharge data to analyze horizontal moisture flux, we have uncovered processes that determine Amur River discharge and their seasonal and interannual variations. Comparison of the moisture flux with the discharge showed that the spring discharge, which peaks in June, is supplied by the moisture flux in the previous autumn and winter. The spring discharge is supplied mainly by short-lived storm activity from the previous autumn and winter. On the other hand, the autumn discharge peak is supplied by the summertime moisture flux. The autumn discharge is supplied mainly by stationary atmospheric patterns in association with the Asian summer monsoon and mid-latitude westerlies.

Interannual variation in the summer moisture flux is related to the strength of the Asian summer monsoon and a stationary anticyclone, the Okhotsk High. The Asian summer monsoon, in association with anomalous cyclonic circulation over Eurasia, strengthens the anomalously large summer moisture flux from the south, resulting in anomalously large discharge in autumn. The Asian winter monsoon, in association with the anomalously strong Siberian High and Aleutian Low, strengthens the moisture flux divergence (*i.e*., activated evaporation in the Amur basin, resulting in anomalously small discharge in spring). The hemispheric atmospheric pattern relates to the moisture flux convergence and, to some extent, resembles the NAM/AO. Anomalously large spring discharge is also related to the warm phase of the NAM/AO, which prompts the melting of snow and frozen soil and thus contributes to the anomalously large spring discharge. Therefore, the NAM/AO pattern influences both the moisture flux and the change in land water storage.

References

Numaguti, A. 1999. Origin and recycling processes of precipitating water over the Eurasian continent: Experiments using an atmospheric general circulation model. *J. Geophys. Res.* **104**: 1957–1972, doi:10.1251029/1998JD200026.

Ogi, M. and Tachibana, Y. 2006. Influence of the annual Arctic Oscillation on the negative correlation between Okhotsk Sea ice and Amur River discharge. *Geophys. Res. Lett.* **33**: L08709, doi:10.1029/2006GL025838.

Ogi, M., Tachibana, Y., Nishio, F. and Danchenkov, M. A. 2001. Does the fresh water supply from the Amur river flowing into the Sea of Okhotsk affect sea ice formation? *J. Meteor. Soc. Japan* **79**: 123–129.

Oshima, K. and Yamazaki, K. 2006. Difference in seasonal variation of net precipitation between the Arctic and Antarctic regions. *Geophys. Res. Lett.* **33**: L18501, doi:10.1029/2006GL027389.

Tachibana, Y., Oshima, K. and Ogi, M. 2008. Seasonal and interannual variations of Amur River discharge and their relationships to large-scale atmospheric patterns and moisture fluxes. *J. Geophys. Res.* **113**: D16102, doi:10.1029/2007JD009555.

Uppala, S.M. *et al.* 2005. The ERA-40 reanalysis. *Quart. J. Roy. Meteorol. Soc.* **131**: 2961–3012, doi:10.1256/QJ.04.176.